 doi:10.20944/preprints202208.0369.v1

Article

Overexpressed C-Myc Sensitize Cells to TH1579, an Mitotic Arrest and Oxidative DNA Damage Inducer

Sofia Henriksson[1¶], José Manuel Calderón-Montaño[2¶], Daniel Solvie[3], Ulrika Warpman Berglund[1,4] and Thomas Helleday[1,*]

[1]Science for Life Laboratory, Department of Oncology-Pathology, Karolinska Institutet, 171 65 Stockholm, Sweden; henriksson.sofia@icloud.com; ulrika.warpmanberglund@ki.se; Thomas.Helleday@scilifelab.se;
[2]Department of Pharmacology, Faculty of Pharmacy, University of Seville, 41012 Seville, Spain; jcalderon@us.es

[3] Theodor Boveri Institute, Department of Biochemistry and Molecular Biology, Biocenter, University of Würzburg, 97070, Würzburg, Germany ; daniel.solvie@uni-wuerzburg.de

[4]Oxcia AB, Norrbackagatan 70C, SE113 34 Stockholm, Sweden; ulrika.warpmanberglund@oxcia.com

* Correspondence: Thomas.helleday@scilifelab.se ; Tel.: (optional; include country code; if there are multiple corresponding authors, add author initials)

Abstract: Previously, we reported that MTH1 inhibitors TH588 and TH1579 selectively induce oxidative damage and kill Ras expressing or transforming cancer cells, as compared to non-transforming immortalized or primary cells. While this explains the impressive anti-cancer properties of the compounds, the molecular mechanism remains elusive. Oncogenes induce replication stress, resulting in under replicated DNA and replication continuing into mitosis, where TH588 and TH1579 treatment cause toxicity and incorporation of oxidative damage. Hence, we hypothesized that oncogene-induced replication stress explains the cancer selectivity. To test this, we overexpressed c-Myc in human epithelial kidney cells (HA1EB), resulting in increased proliferation, polyploidy and replication stress. TH588 and TH1579 selectively kill c-Myc overexpressing clones, enforcing the cancer cell selective killing of these compounds. Moreover, the toxicity of TH588 and TH1579 in c-Myc overexpressing cells is rescued by transcription, proteasome or CDK1 inhibitors, but interestingly not by nucleoside supplementation. This suggest that cancer selectivity is unrelated oncogene-induced replication stress. We conclude that the molecular toxicological mechanisms how TH588 and TH1579 kill c-Myc overexpressing cells have several components and involves MTH1-independent proteosomal degradation of c-Myc itself, c-Myc driven transcription and CDK activation, and is likely unrelated to oncogene-induced replication stress.

Keywords: MTH1; TH588; TH1579; c-Myc; replication stress; DNA damage; cell death; cancer

1. Introduction

In our lab, we generated MTH1 inhibitors TH588 and TH1579 and showed that these have anti-cancer properties selectively killing off transforming cancer cells and being well tolerable in non-transformed cells(1, 2). Currently, TH1579 is evaluated in several clinical trials (Eudnr 2016-00262480 and 2019-001221-27) and here we wanted to understand the molecular mechanism for the cancer selectivity of TH588 and TH1579. TH588 and TH1579 act via a dual mechanism, i) causing mitotic arrest by disturbing microtubule polymerisation (3) (likely both dependent and independent on MTH1 (4)), which altogether increasing ROS, and ii) promoting the incorporation of 8-oxodGTP into DNA during mitotic replication by inhibiting MTH1 and thus causing cell death(4, 5). In humans, the MTH1 enzyme is involved in protection against reactive oxygen species (ROS) where it hydrolyzes oxidized dNTPs, such as 8-oxodGTP into 8-oxodGMP, preventing the incorporation of this oxidized nucleotide into DNA(6). Moreover, recent data has shown that the MTH1 protein binds tubulin, promotes microtubule polymerization and mitotic progression to avoid oxidative DNA damage(4). Different MTH1 inhibitors differentially affect microtubule polymerization. TH588 and TH1579 cause incorporation of oxidized dNTPs during

 doi:10.20944/preprints202208.0369.v1

mitosis in mitotic replication, an effect linked to MTH1 inhibition (5). Mitotic replication is essentially a repair synthesis process of lesions, caused by replication stress occurring in S-phase, that then are carried over to G2/M and repaired by processes such as homologous recombination (7, 8). The objective in this study is to understand the molecular reason(s) by which TH588 and TH1579 can kill cancer but not non-transformed cells. Our hypothesis is that cancer cells are sensitive to these inhibitors owing to high level of oncogene-induced replication stress (9, 10), resulting in chromosomal instability(11), and what we hypothesize repair synthesis incorporating 8-oxodGTP in cancer cells. There are previous reports linking replication stress to oxidative stress, activating DNA damage response in gliomas(12).

Here, we wanted to generate an isogenic system to study the effect of oncogene-induced replication stress on response to TH588 and TH1579. The single oncogene that is amongst those that most efficiently induce DNA replication fork stress is the transcription factor c-Myc (13, 14). In addition to c-Myc, the Myc family includes N-Myc and L-Myc, which all belong to the helix-loop-helix/leucine zipper class of transcription factors. The expression of the Myc family is controlled under normal conditions and coordinates many biological processes, such as cell cycle progression, metabolism, DNA replication and more. The Myc family is deregulated in at least 40% of human cancers and this deregulation is frequently associated with poor prognosis and unfavorable survival in patient with cancer such as renal cancer, urothelial cancer and ovarian cancer (15, 16). Previous studies have described c-Myc both as a transcriptional and non-transcriptional regulator of DNA replication, via stimulating components driving the cell cycle and through interaction with the pre-replicative complex increasing the number of firing replication origins (13, 17). Collisions between replication-transcription complexes, alterations of nucleotide pools or metabolic processes resulting in increased levels of reactive oxygen species (ROS) that induce DNA damage have been suggested to contribute to c-Myc-induced replicative stress (14). The increased load of ROS observed in cancer can result in direct oxidation of DNA or, preferentially, cause damage within the free dNTP pool. One of the major products of nucleotide oxidation is 8-oxo-2′-deoxyguanosine-triphosphate (8-oxodGTP) that upon mispairing with adenine once incorporated into DNA, results in mutations and cell death.

Here, we decided to study the effect of c-Myc overexpression on sensitivity following TH588 or TH1579 treatment. Our results show that cells overexpressing c-Myc accumulate in S phase, have slower replication fork speed and suffer from replication stress. Moreover, these cells are sensitive to TH588 and TH1579 and the levels of c-Myc drastically drop following TH588 or TH1579 treatment. The lost viability could be rescued by addition of transcriptional, proteasomal and CDK1 inhibitors, most likely via different signaling pathways. This indicates that c-Myc overexpression induces sensitivity to TH588 or TH1579 treatment, which could be used clinically especially in cancers with known c-Myc deregulation such as aggressive prostate cancer, ovary cancer and breast cancer (18).

2. Materials and Methods

Cells and culture conditions

Human immortal, non-tumorigenic HA1EB cells were cultured in Dulbecco's modified Eagle's medium (Gibco, ThermoFisher) supplemented with 10% fetal bovine serum and Pen/Strep in a humidified CO_2 atmosphere at 37°C. The c-Myc overexpressing cells and the control cells (empty vector) were generated by stable transfection with PB-GFP or PB-GFP-cMYC (pHULK piggyBac Mammalian Expression Vectors as previously described(19)

Drug treatments

 doi:10.20944/preprints202208.0369.v1

Compounds used in this study include: cordycepin (Sigma-Aldrich; cat# **C3394)**, RO-3306 (Sigma-Aldrich; cat# **SML0569**), Mitomycin C (Sigma-Aldrich; cat# M4287), bortezomib (Selleckchem, cat# PS-341), dNTPs (Sigma-Aldrich; cat# U3003, C4654, G6264, A4036). TH588 and TH1579 were synthesized in house, whereas AZ19 compound was provided by AstraZeneca.

Transfection

Cell were grown in either 6-well or 96-well plate setup with a seeding density of 50.000 cells or 1.500 cells per well respectively. 24 h after seeding, the cells were transfected using 10 nM siRNA. INTERFERin® (Polyplus; cat#409-10) was used as transfection reagent. As negative control AllStars Negative control siRNA (QIAGEN, cat# SI03650318) was used. To avoid starvation in a 96-well plate setup, 24 h after transfection 50 µl serum containing media was added. The following MTH1 siRNA sequence was used: 5'-CGACGACAGCUACUGGUUU-3' (siMTH1#3).

Antibodies

The following antibodies were used in this study: mouse anti-β-actin (Abcam; cat# ab6276), mouse anti-γH2AX-S139 (Millipore; cat# 05-636), mouse anti-c-Myc (Santa Cruz; cat# sc-42, Santa Cruz), rabbit anti-Cleaved PARP Asp214 (Cell Signaling; cat# 9541), rabbit anti-MTH1 (Novus Biologicals; cat# NB100-109), rabbit anti-p53 pS15 (Cell Signaling; cat# 9284), mouse anti-p53 (Santa Cruz; cat# sc-126), mouse anti-GAPDH (Abcam; cat# ab8245), rat anti-RPA32 (Cell Signaling; cat# 2208).

The secondary antibodies used: goat anti-rat Alexa Fluor® 568 (Life Technologies; cat# A-11077), goat anti-rat Alexa Fluor® 647 (Life Technologies; cat# A-21247), IRDye® 800CW donkey anti-rabbit (LI-COR; cat# 926-32213), IRDye® 680RD donkey anti-rabbit (LI-COR; cat# 926-68073), IRDye® 800CW donkey anti-mouse (LI-COR; cat# 926-32212), IRDye® 680RD donkey anti-mouse (LI-COR; cat# 926-68072).

DNA fiber analysis

HA1EB cells were pulse-labeled with 25 µM CldU for 20 min, washed with medium and pulse-labeled with 250 µM IdU for 30 min. Labeled cells were harvested and DNA fiber spreads were prepared as described elsewhere(20). CldU was detected by incubating acid-treated fiber spreads with rat anti-BrdU monoclonal antibody (Abcam; cat# ab6326), whereas IdU was detected using mouse anti-BrdU monoclonal antibody (BD Biosciences; cat# 347580) for 2.5 hours at RT. Slides were fixed with 4% PFA and incubated with goat anti-rat Alexa Fluor 555 or goat anti-mouse Alexa Fluor 488 for 1.5-2 hours. Fibers were examined using a Zeiss (Jena, Germany) LSM710 confocal laser scanning microscope with a 63x oil immersion objective. For quantification of replication structures, at least 250 structures were counted per experiment. The lengths of red (AF 555) or green (AF 488) labeled patches were measured using the ImageJ software (National Institutes of Health; http://rsbweb.nih.gov/ij/) and arbitrary length values were converted into micrometers using the scale bars created by the microscope.

EdU incorporation

Cells were incubated in media supplemented with 10 µM EdU for 15 min, washed in PBS and then fixed using 4% PFA, 0.1% Triton-X in PBS at RT for 15 min. EdU incorporation was visualized using Click-iT® EdU Alexa Fluor® 594 Imaging Kit (Life Technologies; cat# C10337) according to manufacturer's instructions. Cells were counterstained with DAPI before imaging.

Immunofluorescence microscopy

Cells were grown on coverslips, fixed with 4% PFA for 15 min and permeabilized with 0.1% Triton-X-100 for 5 min. Cells were kept in blocking buffer for 1 hour (2% BSA,

 doi:10.20944/preprints202208.0369.v1

5% glycerol, 0.2% Tween20, 0.1% NaN_3), followed by 1 hour incubation in primary antibody and 30 minutes in secondary antibody. DNA was stained with DAPI and mounted using ProLong® Gold Antifade Mountant (Molecular Probes; cat# P36934). Imaging was carried out using a Zeiss LSM710 confocal laser scanning microscope and Zen software (2012). For RPA32 immunostainings, cells were pre-extracted with 0.1% Triton X-100 for 30 seconds prior to fixation. Samples were incubated overnight with rat anti-RPA32 and 1 h with goat anti-rat Alexa Fluor® 647.

Flow cytometry

Cells were harvested, washed in PBS and fixed in 70% ethanol for 60 min at -20°C or stored until analyzed. Cell were stained in PBS containing 5 µg/ml 7-AAD (7-amino-actinomycin D), 20 µg/ml RNase A and 0.1% Triton X-100 for 1 hour in 4°C. Cell cycle profiles were analyzed using a Navios flow cytometer (Beckman Coulter) and Kaluza analysis software (version 1.2).

qRT-PCR

The Direct-zol™ RNA MiniPrep kit (Zymo Research; cat#R2052) was used to isolate RNA from cultured cells. cDNA was synthesized using the QuantiTect® Reverse Transcription kit (QIAGEN; cat#205313) with 400 ng RNA as starting material. The iTaq Universal SYBR Green Supermix (BioRad; cat#172-5085) was used to perform qRT-PCR with a CFY96 real-time PCR machine (BioRad). Relative expression on mRNA level was calculated in comparison to GAPDH and β-actin. Primer sequences can be found in the supplementary material (Table 1).

Western blotting

Cells were harvested, washed in PBS and proteins were extracted in lysis buffer containing 100 mM Tris-HCL at pH 8, 150 mM NaCl, 1% NP-40 supplemented with phosphatase and protease inhibitors, for 30 min on ice. Protein concentrations were determined using Pierce™ BCA protein assay kit (Thermo Fisher Scientific; cat# 23227) and Western blotting was carried out according to standard protocols.

Resazurin assay

Cells were seeded in 96-well plates (1500 cells/well) and treated with the indicated drugs and doses. 10 µg/ml resazurin was then added to the cells for 4 hours before analysis using a Hidex Sense microplate reader. The absorbance was normalized against background levels and the data processed in Microsoft Excel.

Clonogenic survival assays

1000 cells/ml were seeded in a 6-well plate setup and treated immediately. After 48 h incubation, media containing vehicle or inhibitor were replaced with fresh media and continuously incubated for 5-6 days. Before manual counting of colonies, 4% methylene blue in MeOH was utilized to fix and stain the cells.

Statistical analysis

Statistical significance was determined via two tailed Student's *t*-test using Microsoft Excel. The results originate from at least two independent experiments and are presented as mean ± standard error of the mean (S.E.M).

3. Results

3.1. Generating and characterizing c-Myc overexpressing HA1EB cells

In order to study the direct effects of c-Myc overexpression, we generated HA1EB cell lines that stably expressed full-length c-Myc. HA1EB cells are derived from human

 doi:10.20944/preprints202208.0369.v1

epithelial kidney cells, immortalized via SV40 large T antigen and hTERT expression. In general, these cells are considered genetically stable and can only form tumors if they are transformed by an oncogene (21, 22). Following GFP-tagged plasmid transfection (empty or c-Myc expressing vectors) as described elsewhere(19), cells were selected by flow cytometry and grown from the single-cell level into several different clones (Figure S1A). The selected clones (termed #1-4) were screened for c-Myc expression compared to the empty vector control. Indeed, all four selected clones carried high c-Myc expression both on mRNA and protein level compared to control cells (Figure 1A and 1B). Moreover, levels of endogenous c-Myc mRNA was decreased (Figure S1B), which is in line with previous published data, where exogenous c-Myc negatively regulates endogenous c-Myc mRNA expression (23). Next, we studied the mRNA levels of MTH1 in the HA1EB cells and found no significant difference between empty vector and c-Myc overexpressing cells (Figure S1C). However, the known target of c-Myc, cyclin E1, displayed higher mRNA levels following c-Myc overexpression using clones 3 and 4 as representative models (Figure S1D). Altogether, this data prompted us to continue the investigation of these cell lines as models for response following induced c-Myc overexpression.

We started by studying the cellular proliferation rates in the c-Myc overexpressing cell lines compared to their respective controls. The c-Myc overexpressing cells proliferated much faster than control cells, clearly visible following 72 hours (Figure 1C). Next, we studied the cell cycle profile of the c-Myc overexpressing cells. All four c-Myc overexpressing clones had less G1 content, whereas the cells in S phase increased compared to the cells expressing empty vector (Figure 1D). All four c-Myc overexpressing cell lines experienced more endogenous cell death compared to the control cells (Figure 1E). Subsequently, the amount of polyploid cells was determined and we found that the c-Myc overexpressing cells showed an accumulation of these cells compared to control HA1EB cells (Figure 1F). c-Myc overexpression correlated with cleaved PARP1, phosphorylated p53 and increased γH2AX signaling (Figure S1E), indicating induction of DNA damage and increased cell death upon overexpression of c-Myc alone.

Preprints (www.preprints.org) | NOT PEER-REVIEWED | Posted: 22 August 2022 doi:10.20944/preprints202208.0369.v1

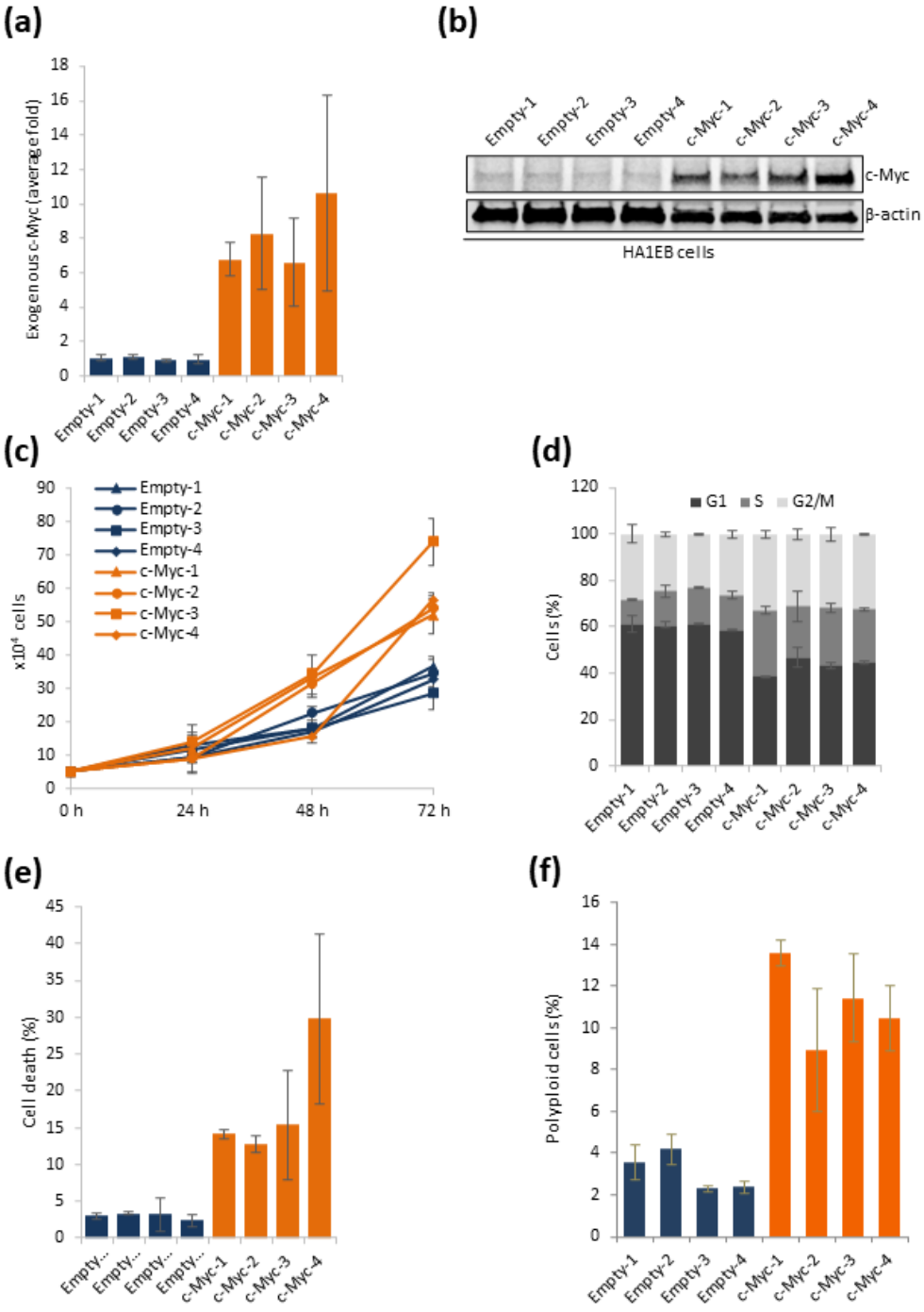

Figure 1. HA1EB cells overexpressing c-Myc proliferate faster. (A) Exogenous c-Myc mRNA levels in HA1EB cells, n=3 ± S.E.M (B) Exogenous c-Myc protein expression in HA1EB cells. (C) HA1EB cells were seeded and counted daily, n=2 ± S.E.M. (D) Cell cycle profiles of HA1EB cells, n=2 ± S.E.M. (E-F) HA1EB cells were seeded and left to grow for 72 hours. Then, cells were harvested, stained with 7-AAD and analyzed using FACS. Dead cells (E), <2N DNA content, and polyploid cells (F), >4N DNA content, n=2 ± S.E.M.

3.2. c-Myc overexpression results in EdU and RPA32 accumulation

Since the c-Myc overexpressing cells accumulated in S phase, we wanted to study DNA synthesis and the replication response in these cells. First, we measured incorporation of the thymidine analogue 5-ethynyl-2′-deoxyuridine (EdU). As expected by the cell cycle profile, the EdU-positive cell population was higher in the cells overexpressing c-Myc compared to the control cells (Figure 2A, 2B and 2C). Moreover, we could detect

Preprints (www.preprints.org) | NOT PEER-REVIEWED | Posted: 22 August 2022 doi:10.20944/preprints202208.0369.v1

more single-stranded DNA (ssDNA) accumulation upon staining cells using RPA32 in the c-Myc overexpressing cells compared to empty control cells (Figure 2A, 2B and 2D). Strikingly, the co-localization of EdU and RPA32 was clearly induced in the HA1EB cells overexpressing c-Myc compared to the control cells (Figure 2E). Overall, this data reveals potential replication fork stalling following the visualization of RPA32 accumulation in S phase cells.

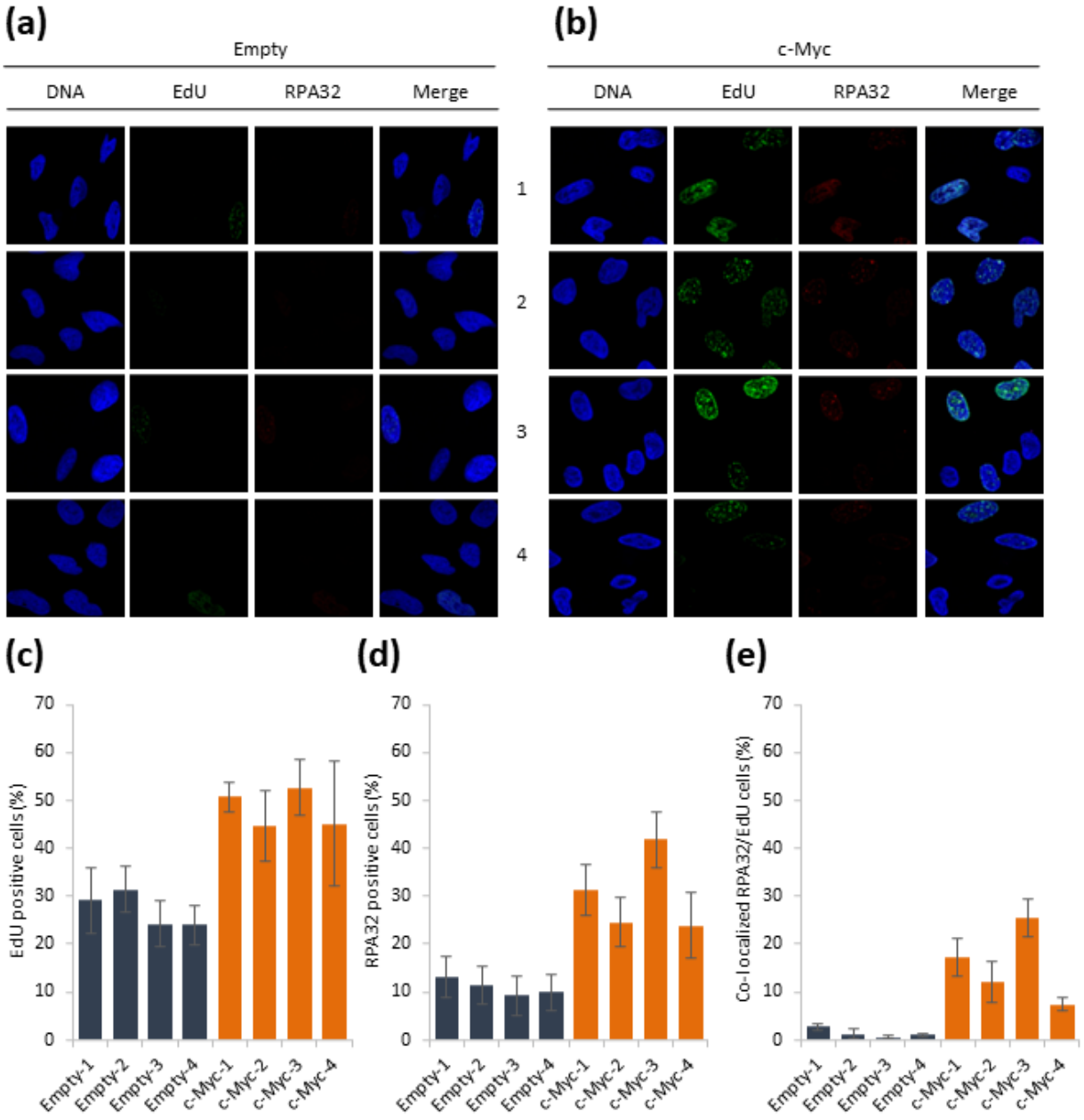

Figure 2. Increased EdU incorporation and RPA32 foci in c-Myc overexpressing HA1EB cells. (A-B) HA1EB cells were labeled with EdU for 15 min and stained with EdU Click-iT (according to the manufacturer's instructions) and anti-RPA32 antibody. DNA was stained using DAPI. Images were taken using a Zeiss LSM-780 confocal microscope and analyzed using Image J software. A total of 150 cells/sample was counted, n=3 ± S.E.M. (C) Quantification of EdU incorporation. Mean intensity ≥5 AU was considered as positive. (D) Percentage of cells with ≥5 RPA32 foci. (E) Percentage of cells with ≥5 RPA32/EdU co-localized foci.

 doi:10.20944/preprints202208.0369.v1

3.3. Excess of c-Myc induces replication stress

In order to directly test if the HA1EB cells overexpressing c-Myc presented replication stress, we performed the DNA fiber assay. Cells were pulse-labelled with CldU for 20 min, followed by washing and a second pulse of IdU for 30 min (Figure 3A, schematic illustration). Thereafter, labelled cells were harvested and the DNA fiber assay was performed. Indeed, the c-Myc overexpressing cells showed significantly shorter DNA fibers compared to control cells (Figure 3A, 3B, 3C and 3D), indicative of replication stress. To determine whether c-Myc overexpression induced fork collapse, we quantified the CldU/IdU ratios. A CldU/IdU value close to 1 means an equivalent fork progression rate during both labelling periods, so perfect fork symmetry; whereas values higher than 2 means fork asymmetry and fork stalling during the second labelling. The c-Myc overexpressing cells did not show significant differences compared to control cells, with average CldU/IdU ratio close to 1-1.5 (Figure 3E), except for the c-Myc-3 clone. These results disagree with those obtained in previous publications(17, 24), where higher degree of fork asymmetry in c-Myc overexpressing cells has been observed. This discrepancy could be due to the differences in experimental design, since we grew our cells for months in order to obtain our clones, which could give the cells enough time to adapt to the c-Myc-induced replication stress. Indeed, it is know that c-Myc overexpression is lethal for the cells if they do not develop mechanisms to compensate and reduce the consequences of replication stress as, for example, DNA double-strand breaks(25). Finally, we quantified the number of firing replication origins. Origins that fired during the first labelling period have a continuous IdU-CldU-IdU tracks (green-red-green signal)(26). It is known that c-Myc overexpression is associated with an excess number of active replication origins to support the acceleration of the S-phase(25). Consequently, c-Myc overexpressing cells showed higher number of first label origins than control cells (Figure 3F). Altogether, these results support that HA1EB cells overexpressing c-Myc suffer from replication stress.

Preprints (www.preprints.org) | NOT PEER-REVIEWED | Posted: 22 August 2022 doi:10.20944/preprints202208.0369.v1

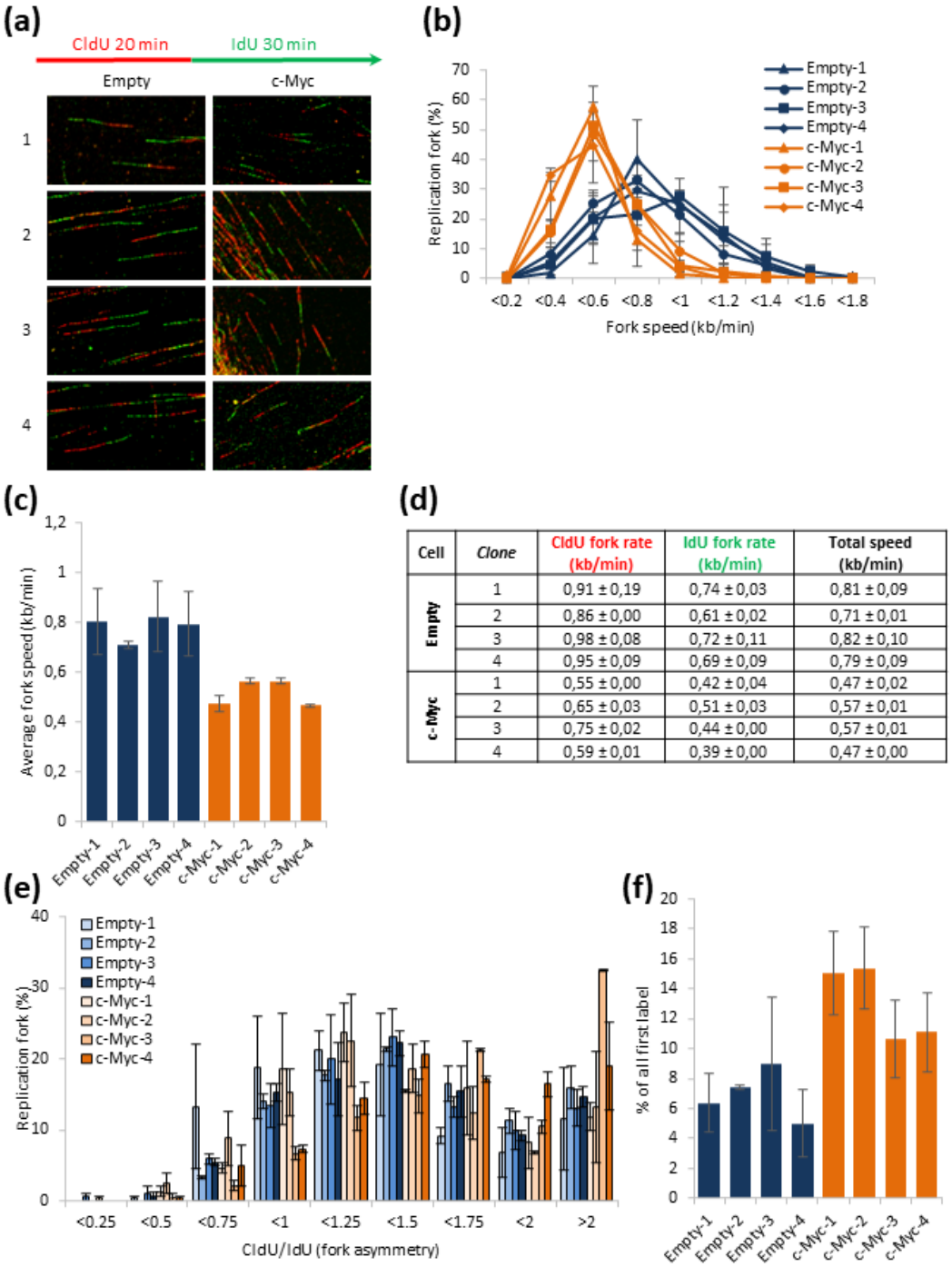

Cell	Clone	CldU fork rate (kb/min)	IdU fork rate (kb/min)	Total speed (kb/min)
Empty	1	0,91 ± 0,19	0,74 ± 0,03	0,81 ± 0,09
	2	0,86 ± 0,00	0,61 ± 0,02	0,71 ± 0,01
	3	0,98 ± 0,08	0,72 ± 0,11	0,82 ± 0,10
	4	0,95 ± 0,09	0,69 ± 0,09	0,79 ± 0,09
c-Myc	1	0,55 ± 0,00	0,42 ± 0,04	0,47 ± 0,02
	2	0,65 ± 0,03	0,51 ± 0,03	0,57 ± 0,01
	3	0,75 ± 0,02	0,44 ± 0,00	0,57 ± 0,01
	4	0,59 ± 0,01	0,39 ± 0,00	0,47 ± 0,00

Figure 3. c-Myc overexpression induces replication stress. (A-F) Cells were seeded and left to grow for 48 hours. After that, cells were labeled for 20 minutes with CldU, washed and labeled with IdU for 30 minutes. Finally, cells were harvested and the DNA fibers were obtained. DNA containing CldU was stained in red and DNA containing IdU was stained in green. The length of individual, well spread labeled fibers was measured and converted into kb/min. Quantitative data presented as means, n=2 ± S.E.M. (A) Schematic illustration of CldU (red) and IdU (green) labelling during the assay and representative images of replicative fork tracks for control cells (HA1EB Empty) and c-Myc overexpressing cells (HA1EB c-Myc). (B) Graph shows the distribution of fork progression speed (kb/min) of the first and second pulses. (C) Average of the replication fork extension rates during the first and the second pulses. (D) Quantification of the mean replication fork speed (kb/min) during the first (CldU, 20 min), the second (IdU, 30 min) and both pulses. (E) Distribution of CldU/IdU ratio of replication fork progression. The value equal 1 means the extension speed was similar during both pulses (perfect symmetry). (F) First label origins (green-red-green) are shown as percentage of all red (CldU) labeled tracks.

 doi:10.20944/preprints202208.0369.v1

3.4. TH588 or TH1579 treatment decreases viability of c-Myc overexpressing cells

Having established that our HA1EB cells overexpressing c-Myc displayed the expected phenotype, we decided to test if these cells were sensitive to TH588 or TH1579 treatment. We treated all eight cell lines with varying concentrations of MTH1 inhibitors, TH588 (Figure 4A) and TH1579 (Figure 4B). Following 72 hours, both MTH1 inhibitors showed higher cytotoxicity against c-Myc overexpressing cells than control cells (Figure 4A and 4B). Next, we decided to scale down the experiments and focus on two different cell lines, clones 3 and 4, used in the clonogenic survival experiments of control and c-Myc overexpressing cells following MTH1 inhibitor treatment. The c-Myc-4 overexpressing cells displayed a clear decrease in surviving clones, going down to zero colonies following MTH1 inhibitor treatment (Figure 4C and 4D). Conversely, the control cells were basically unaffected at the concentration used (Figure 4C and 4D). Similar results were found in c-Myc-3 cells (data not shown). Finally, we depleted MTH1 using siRNA in order to see if the observed toxic effect was specific to the MTH1 inhibitors or not. The knockdown appeared to function well following 72 hours (Figure S2A). At that timepoint, the viability of c-Myc overexpressing cells was also decreased (Figure 4E and 4F), but not as intensely as compared to the MTH1 inhibitors.

Preprints (www.preprints.org) | NOT PEER-REVIEWED | Posted: 22 August 2022 doi:10.20944/preprints202208.0369.v1

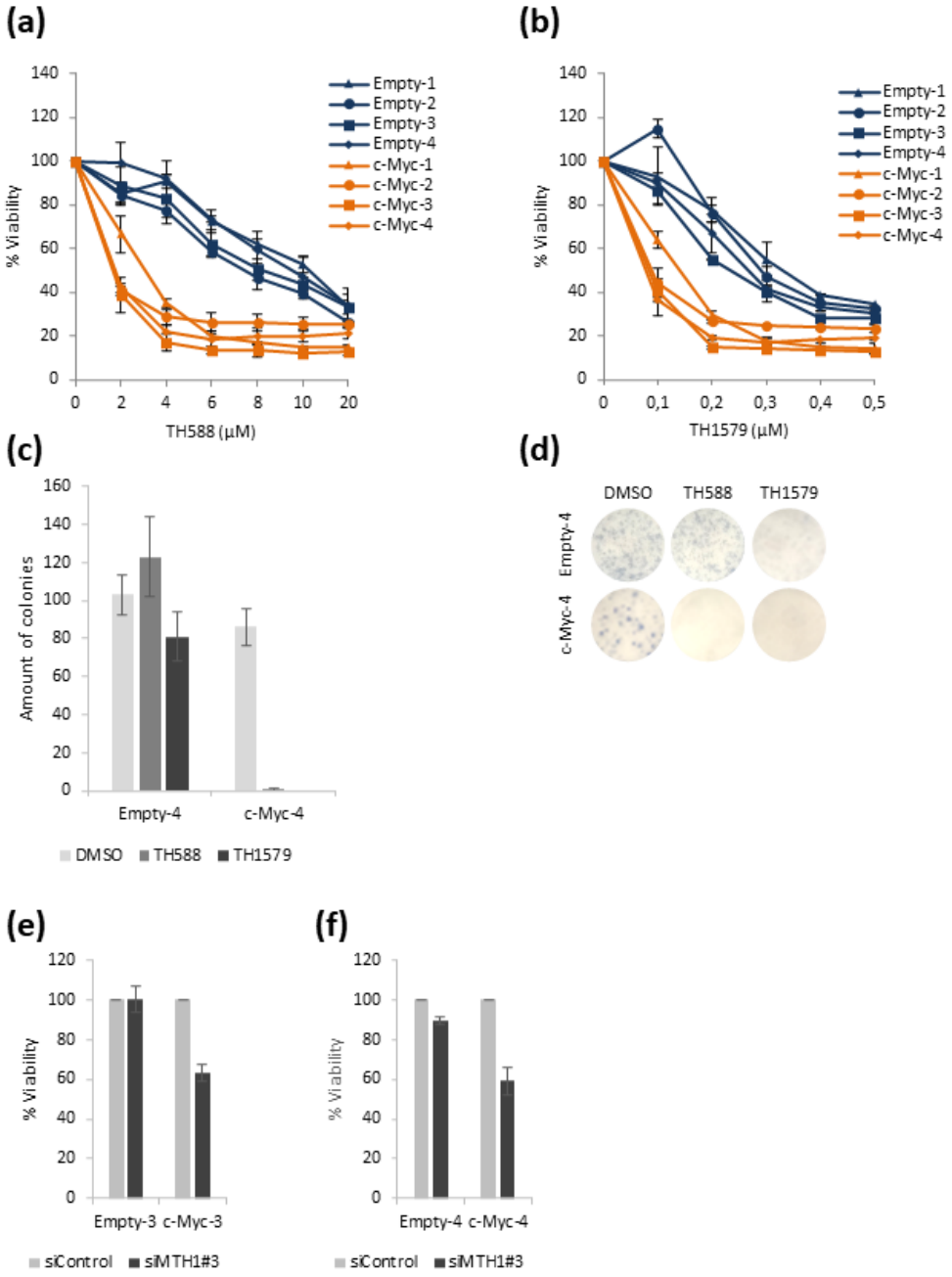

Figure 4. Viability of c-Myc overexpressing cells is decreased upon TH588 or TH1579 treatment or MTH1 silencing. (A-B) Empty and c-Myc overexpressing cells were plated and treated with the indicated concentrations of TH588 or TH1579 (or DMSO). 72 h later, 10 µg/ml resazurin was added for 4 h and viability was determined (values are normalized to DMSO), n=3 (A) n=2 (B) ± S.E.M. (C) Empty-4 and c-Myc-4 cells were seeded, immediately treated with 5 µM TH588 or 0.5 µM TH1579 for 48 hours, new media was added every 2-3 days until colony staining (9-10 days after seeding). The values were normalized to DMSO control, n=2 ± S.E.M. (D) Representative clonogenic survival assay images of Empty-4/c-Myc-4 cells. (E-F) Cells were seeded and transfected with 10 nM siRNA. 72 hours later, 10 µg/ml resazurin was added for 4 hours and viability was determined (values are normalized to siControl), (E) n=3, (F) n=2 ± S.E.M.

3.5. MTH1 inhibitors TH588 and TH1579 depletes c-Myc protein and cause cell death

 doi:10.20944/preprints202208.0369.v1

In order to determine the toxic mechanism of action of TH588 or TH1579 in c-Myc overexpressing cells, we studied the expression of c-Myc, cleaved PARP1 and γH2AX following 24 hours exposure to TH588 or TH1579. Surprisingly, c-Myc levels drastically dropped following TH588 or TH1579 treatment, which correlated with cleaved PARP1 and γH2AX in the c-Myc overexpressing cells (Figure 5A). This effect overlaps with the reduced survival of cells following TH588 or TH1579 treatment in c-Myc overexpressing cells. Next, we studied the effect on the c-Myc mRNA expression following TH588 or TH1579 treatment, but found no significant difference following 24 hours of treatment (Figure S2B). This shows that TH588 and TH1579 only negatively affects c-Myc protein levels and not mRNA levels. After this, we decided to test a non-toxic MTH1 inhibitor, AZ19, originally produced at AstraZeneca(27), to determine its effect on c-Myc levels. We also included mitomycin C (MMC), previously published to reduce c-Myc protein expression levels(28). Interestingly, the non-toxic MTH1 inhibitors did not affect c-Myc levels nor induced γH2AX or PARP1 cleavage (Figure S2C). MMC gave similar c-Myc reduction as TH588 and TH1579, and increased activation of γH2AX and cleaved PARP1 (Figure S2C). Next, we silenced MTH1 expression to determine whether c-Myc levels also decreased using this condition. Although we observed a decreased survival of c-Myc overexpressing cells following MTH1 silencing, we did not observe any drop in c-Myc levels (Figure S2D and S2E) following MTH1 knockdown. However, γH2AX was induced and PARP1 cleaved whereas c-Myc levels appeared to increase upon exposure to MTH1 siRNA. This suggests that loss of MTH1 from cells via RNAi induces reduced cell viability, but not via destabilization of c-Myc protein levels.

Since neither TH588 nor TH1579 affected c-Myc transcription, we reasoned that the treatment may trigger proteolytic degradation of c-Myc. To test this, we used proteasome inhibitor bortezomib which showed some stabilization of c-Myc following TH588 or TH1579 treatment (Figure 5B, which also correlated with no increase in cPARP1 and γH2AX. Following this, we wanted to determine if the lack of c-Myc loss caused by bortozimib also increased the viability. While bortozimib treatment itself was the same in c-Myc overexpressing cells compared to control cells (Figure 5C, we found that co-treatment with bortozimib rescued toxicity induced by TH588 and TH1579 (Figure 5D). These data suggest that one mechanism by which TH588 and TH1579 kill c-Myc overexpressing cells is by degradation of c-Myc itself.

Preprints (www.preprints.org) | NOT PEER-REVIEWED | Posted: 22 August 2022 doi:10.20944/preprints202208.0369.v1

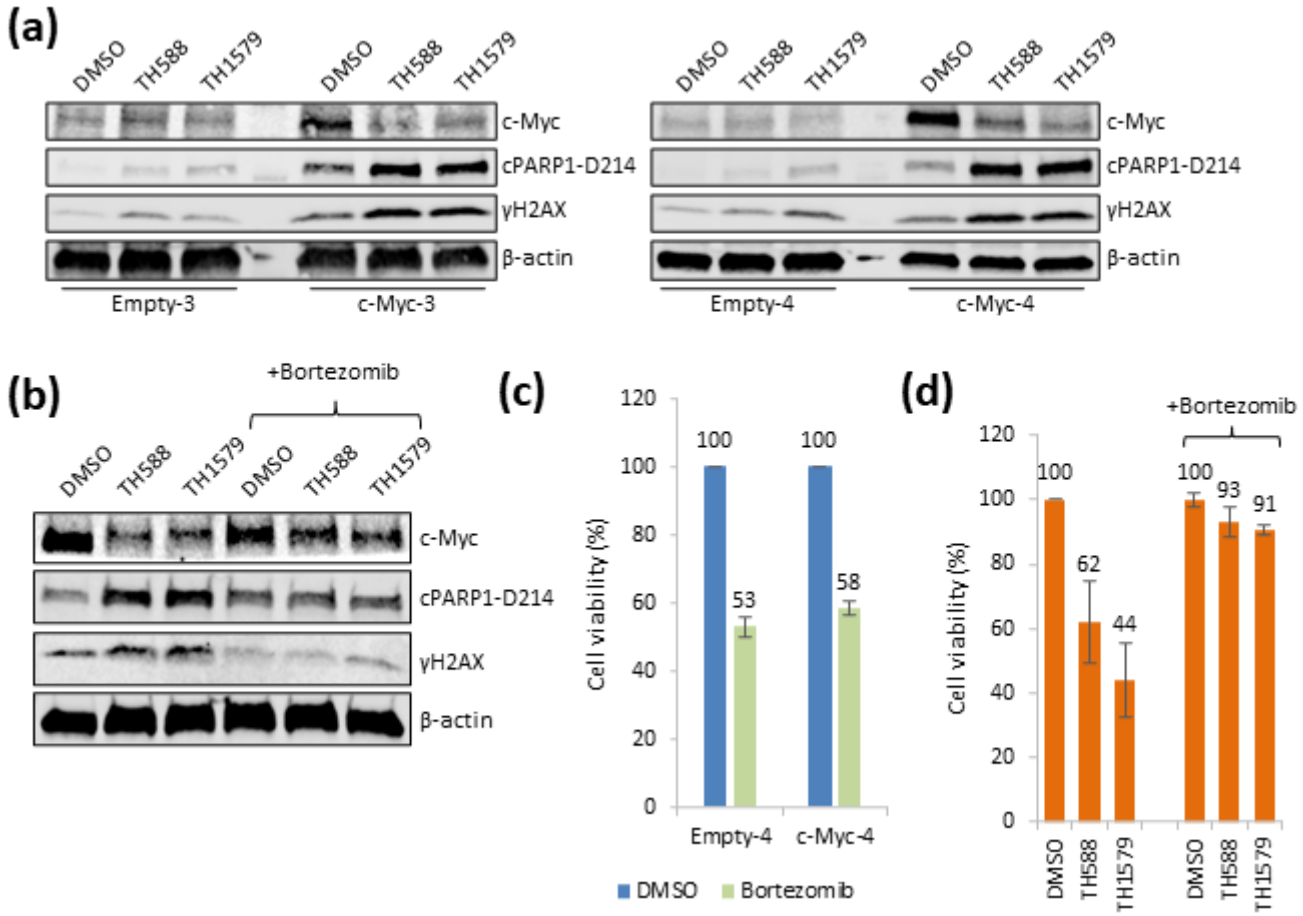

Figure 5. TH588 and TH1579 trigger cell death by degradation of c-Myc protein. A) Empty-3/c-Myc-3 or Empty-4/c-Myc-4 were treated with 5 μM TH588 or 0.5 μM TH1579 for 24 hours. Following cell lysis, the indicated proteins were blotted. (B) c-Myc-4 cells were treated with 5 μM TH588 or 0.5 μM TH1579 for 24 hours ± co-addition of bortezomib (10 nM). The indicated proteins were blotted. (C-D) c-Myc-4 cells were seeded and following 24 hours, the cells were treated with 5 μM TH588 or 0.5 μM TH1579 for 24 hours ± co-addition of bortezomib (10 nM). 10 μg/ml resazurin was added for 4 hours and viability was determined (values are normalized to internal DMSO control), n=2 ± S.E.M.

3.6. Transcription and CDK1 inhibition reverse toxicity of MTH1 inhibitors TH588 and TH1579 in c-Myc overexpressing cells

Here, we established isogenic c-Myc overexpressing cells that have high levels of replication stress. Next, we aimed at determining if we are able to rescuing the toxic effects of TH588 or TH1579 treatment in the c-Myc overexpressing cells by reversing replication stress. We and others have demonstrated that replication stress can be reversed by inhibition of CDK activity (29), inhibition of transcription using cordycepin (30), or addition of nucleosides (11, 31). Here, we used the CDK1 inhibitor RO-3306, cordycepin and nucleoside rescue for 24 hours and monitored c-Myc levels, DNA damage by γH2AX and apoptosis cleaved PARP1 using Western Blotting (Figure 6A). First we explored the toxicity of the selected agents and most of them were more toxic to the c-Myc overexpressing cells compared to control cells, except MG132, dNTPs and bortezomib (Figure S3). We observed no difference in c-Myc levels but reduced levels of both cleaved PARP1 and γH2AX upon addition of nucleosides, RO-3306 or proteosome inhibitor MG132, while the drop of DNA damage (γH2AX) was modest with cordycepin (Figure 6A). The loss of the DNA damage (γH2AX) marker is a clear signal of reduced replication stress, in particular following RO-3306 and nucleoside treatment. In line with the hypothesis that replication stress is related to TH588 and TH1579-induced toxicity in Myc overexpressing cells we

Preprints (www.preprints.org) | NOT PEER-REVIEWED | Posted: 22 August 2022 doi:10.20944/preprints202208.0369.v1

observed that both cordycepin and RO-3306 reversed TH588 and TH1579-induced toxicity (Figure 6B). This is also in line with the observed reduced levels of cleaved PARP and γH2AX. Surprisingly, nucleoside addition did not rescue reduced viability after TH588 or TH1579 treatment (Figure 6B), which is in contrast to the proposed replication stress hypothesis. Since nucleosides reduced TH588 and TH1579-induced γH2AX levels in c-Myc overexpressing cells, we conclude that replication stress levels are not directly linked with sensitivity to TH588 and TH1579.

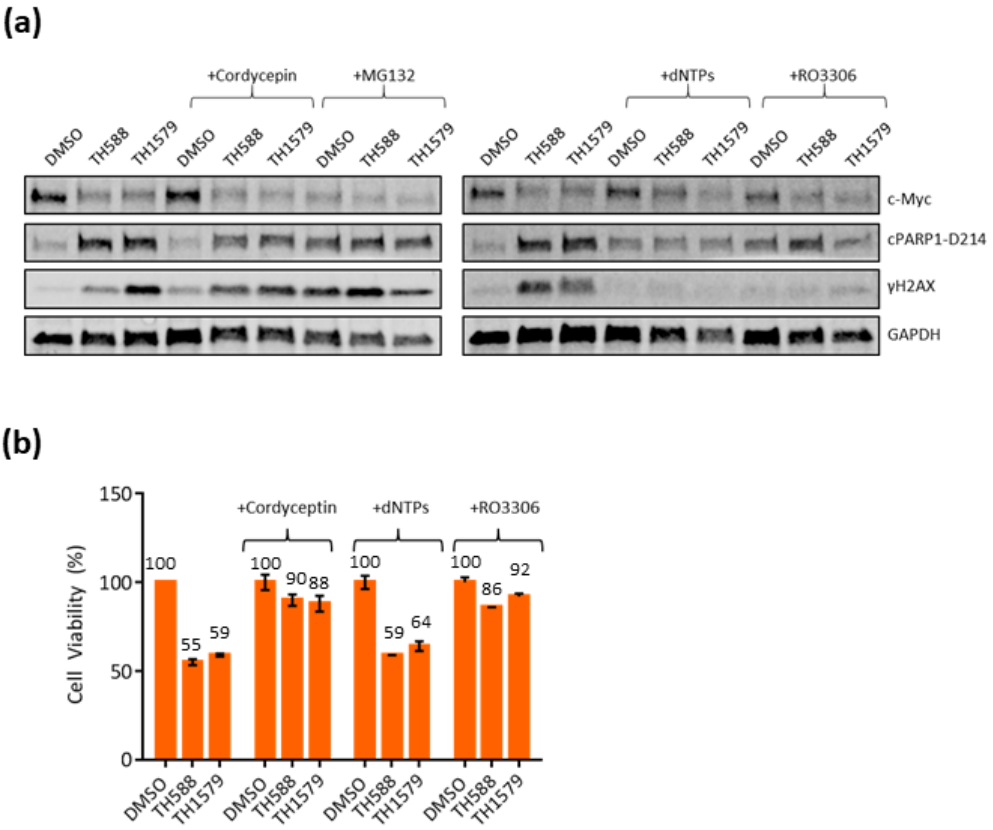

Figure 6. Inhibition of transcription and CDK activity reverse DNA damage and toxicity of MTH1 inhibitors TH588 and TH1579 in c-Myc overexpressing cells. (A) c-Myc-4 cells were treated with 5 μM TH588 or 0.5 μM TH1579 for 24 hours ± co-addition of cordycepin (50 μM), nucleosides (dN) (50 μM) or RO-3306 (5 μM). The indicated proteins were blotted. (B) c-Myc-4 cells were seeded and following 24 hours, the cells were treated with 5 μM TH588 or 0.5 μM TH1579 for 24 hours ± co-addition of cordycepin (50 μM), nucleosides (dN) (50 μM), RO-3306 (5 μM). 10 μg/ml resazurin was added for 4 hours and viability was determined (values are normalized to internal DMSO control), n=2 ± S.E.M.

4. Discussion

In this study, we generated isogenic HA1EB cells overexpressing c-Myc that displayed the expected phenotype associated with oncogene overexpression, i.e., faster proliferation, increased cell death, S phase accumulation and DNA replication stress. Here, we wanted to use this new cell model to determine if c-Myc overexpression are sensitizing these cells to TH588 and TH1579, as previously shown with the Ras oncogene (1). Indeed, we find that Myc overexpressing cells are more sensitive to TH588 and TH1579, accompanied with γH2AX induction and PARP1 cleavage, which would be in line with DNA damage induction and cellular apoptosis previously reported after TH588 or TH1579 treatment.

The second aim was to understand the molecular mechanism sensitizing c-Myc overexpressing cells and we found to our surprise that the levels of c-Myc dropped upon TH588 and TH1579 treatment. Since c-Myc mRNA levels were unchanged and a proteasomal inhibitor bortozemib prevented c-Myc degradation we conclude that TH588 and TH1579 treatment triggers proteasomal degradation of c-Myc. Furthermore, since bortozemib decreases TH588 and TH1579 cell killing we propose that this proteosomal targeting of c-Myc is contributing mechanism to killing these cells. Since c-Myc is considered to be an undruggable target due to its essential cellular functions, it is interesting to identify compounds that indirectly target c-Myc. The MYC family is deregulated in more than 50% of human cancers and is commonly associated with poor prognosis(15). We have also worked with different neuroblastoma cell lines carrying amplified N-Myc and identified that TH588 or TH1579 treatment leads to N-Myc protein abolishment (data not shown). Although we do not know the exact mechanism(s) as to how these inhibitors negatively regulates members of the MYC family, this would be of particular interest for future studies including the status of the Myc/Max complex and other means of destabilizing Myc.

Here, we argue that c-Myc proteolytic degradation by TH588 and TH1579 is unrelated to MTH1 as neither MTH1 siRNA nor the structurally unrelated AZ19 MTH1 inhibitor decreases c-Myc levels. It is established that the TH588 and TH1579 compounds have dual mechanism targeting MTH1 as well as a direct effect on tubulin, and this is an effect likely related to any tubulin effect of the compounds as it also previously has been reported that anti-microtubule drugs results in reduced c-Myc levels (24).

Our original hypothesis was that selective toxicity in cancer cells by TH588 and TH1579 is related to elevated replication stress in cancer. Replication stress is a consequence of collision between transcription and replication (32) and cordycepin reverses replication stress. Here, we find that cordycepin reverses toxicity by TH1579, but it is not clear that this is owing to loss of replication stress as the reduction of γH2AX is only modest. We have also shown that replication stress is reversed by CDK inhibitors (29), and in this case we see both reversed toxicity and reduced DNA damage in line with this hypothesis that replication stress causes toxicity in cancer cells. Finally, as replication stress is also reversed by nucleoside supplementation (31), which is evident also in our setting by reduced γH2AX, it is surprising, and incompatible with our hypothesis, that this does not reverse TH588 nor TH1579-induced toxicity. Altogether, our data does not support our initial hypothesis that replication stress is underlying cancer cell selectivity. An alternative explanation for reversed toxicity with the transcription inhibitor cordycepin could be reduced c-Myc-driven transcription and the effects with the CDK inhibitor related to the role of c-Myc in replication(33).

In conclusion, we have in this study found that oncogenic c-Myc expression functions as a sensitizer to TH588 and TH1579 treatment. We generated an isogenic cell system to have a 'clean' model to single out the effect of c-Myc. Despite this, we find that the molecular toxicological mechanism specifically sensitizing c-Myc overexpressing cells to TH588 and TH1579 is complex and involve, proteasomal degradation of c-Myc, as well as being dependent on c-Myc transcription and CDK activation. While this study reveals a complex toxic mechanism of TH588 and TH1579 killing c-Myc overexpressing cells, which also involve MTH1-independent effects of the compounds, the cancer selective killing of these compounds is confirmed and support further development of TH1579 in the clinic in treatment of cancer.

Author Contributions: Conceptualization, S.H., J.M.C.M, U.WB, T.H.; methodology, S.H, J.M.C.M, D.S.; investigation, S.H, J.M.C.M, D.S.; resources, T.H., U.WB., S.H.; writing—original draft preparation, S.H, J.M.C.M., T.H.; writing—review and editing, U.W.B, T.H..; supervision, UWB, T.H. All authors have read and agreed to the published version of the manuscript.

Funding: This work was supported primarily by grants from The Swedish Childhood Cancer Foundation (S.H.; T.H.), and in addition grants from The Swedish Cancer

 doi:10.20944/preprints202208.0369.v1

Society (T.H.), The Swedish Research Council (T.H.), Torsten and Ragnar Söderberg Foundation (T.H.), the Swedish Foundation for Strategic Research (RB13-0024, U.W.B.).

Acknowledgments: We thank Tobias Koolmeister, Martin Haraldson, and Martin Scobie for synthesis of TH1579 and TH588.

Conflicts of Interest: A patent has been filed with MTH1 inhibitors where T.H., is listed as inventor. The Intellectual Property Right is owned by the non-profit Thomas Helleday Foundation for Medical Research (THF). T.H. and U.W.B are board members of the THF. U.W.B is CEO of Oxcia AB. J.M.C.M, has shares in Oxcia AB. THF is sponsor for ongoing clinical phase 1 trial with TH1579. The other authors declare that there are no conflicts of interest

Appendix B

Supplementary Table 1

Target Gene	F/R	Target Sequence	Reference
Exogenous c-Myc	CMYC_F2	TCGGATTCTCTGCTCTCCT	IDT, Ref. No. 72670694/5
	CYCN_R2	CCTCATCTTCTTGTTCCTCCTC	
Endogenous c-Myc	CMYC_F1	GCTGCTTAGACGCTGGATTT	IDT, Ref. No. 72670696/7
	CMYC_R1	GAGTCGTAGTCGAGGTCATAGTT	
Cyclin E	CCNE_F1	GTCCTGGCTGAATGTATACATGC	Sherr, C.J., Cell, 73, 1059-1065 (1993)
	CCNE_R1	CCCTATTTTGTTCAGACAACATGGC	
MTH1	MTH1_F1	AAAGTGCAAGAAGGAGAGACC	IDT, Ref. No. 72670688/9
	MTH1_R1	CTCGCCCACGAACTCAAA	
GAPDH	hGAPDH_F	AAGGTCGGAGTCAACGGATT	M.Altun (Hassink et al., 2009)
	hGAPDH_R	CTCCTGGAAGATGGTGATGG	
β-Actin	hb-actin_F	CCTGGCACCCAGCACAAT	M.Altun (Hassink et al., 2009)
	hb-actin_R	GGGCCGGACTCGTCATACT	

Preprints (www.preprints.org) | NOT PEER-REVIEWED | Posted: 22 August 2022 doi:10.20944/preprints202208.0369.v1

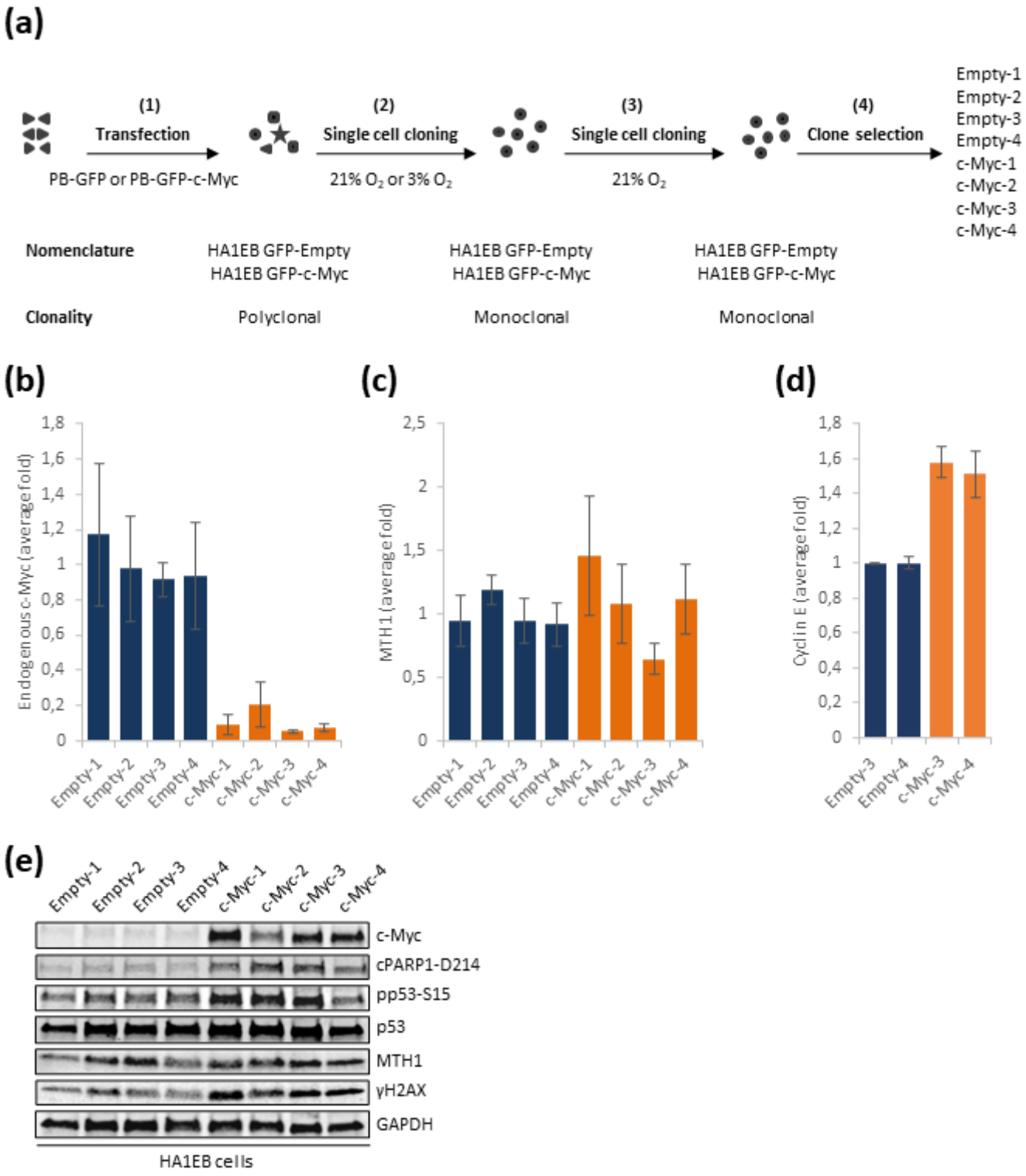

Figure S1. Schematic illustration of cell line generation and marker levels in c-Myc HA1EB cells. (A) After transfection with PB-GFP vector (encoding GFP) or PB-GFP-c-Myc vector (encoding GFP and c-Myc), GFP positive cells were selected by FACS (1). Then, cells were seeded to obtain single-cell clones and incubated in normoxia (21% O_2) or hypoxia (3% O_2) (2). Single-cell clones derived from the polyclonal population were isolated and reseeded for a second single-cell cloning step. The cells were kept in normoxia (3). c-Myc levels were analyzed at each stage by Western blot. The final single-cell clones were used for analysis of replicative profiles. (B) HA1EB Empty and c-Myc over-expressing cells analyzed for endogenous c-Myc mRNA levels (targeting 5′UTR). (C) MTH1 mRNA

 doi:10.20944/preprints202208.0369.v1

levels in HA1EB cells. (D) Cyclin E1 mRNA levels in Empty-3/4 and c-Myc-3/4 cells, (B-D) n=3. (E) Levels of the indicated proteins in HA1EB cells.

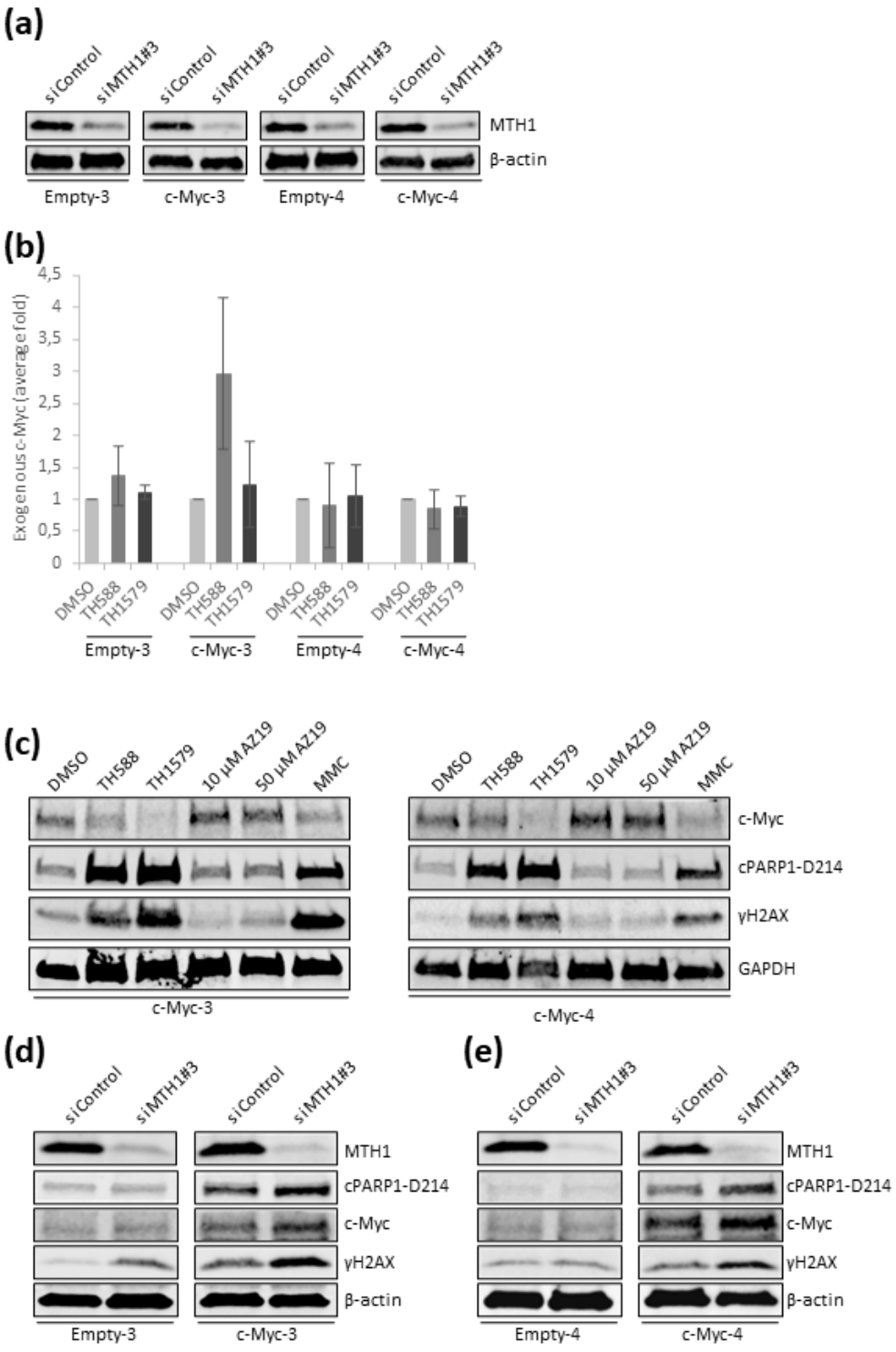

Figure S2. Non-toxic MTH1 inhibitors or MTH1 silencing do not decrease c-Myc levels. (A) HA1EB cells (Clones 3 and 4), were transfected with 10 nM siRNA for 72 hours followed by blotting for the indicated proteins. (B) Exogenous c-Myc mRNA levels were measured 24 hours post 5 μM TH588 or 0.5 μM TH1579 in HA1EB cells (Clones 3 and 4), n=2 ± S.E.M. (C) c-Myc-3 and -4 cells were treated with 5 μM TH588, 0.5 μM TH1579, 10 μM AZ19, 50 μM AZ19 or 4 μg/ml mitomycin C (MMC) for 24 hours. The indicated proteins were studied. c-Myc-3 (D) or c-Myc-4 (E) were transfected with 10 nM siRNA, harvested 72 hours later and the expression of indicated proteins was analyzed.

 doi:10.20944/preprints202208.0369.v1

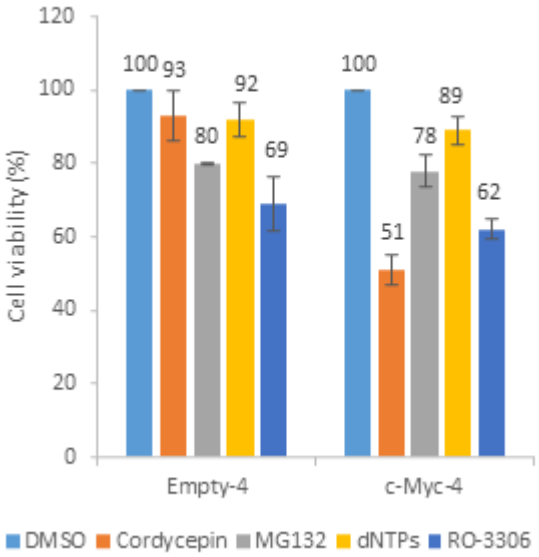

Figure S3. Toxicity of used inhibitors in Empty-4 and c-Myc-4 HA1EB cell lines. (A-B) Empty-4 and c-Myc-4 cells were seeded and following 24 hours, the cells were treated with DMSO ± co-addition of cordycepin (50 μM), , dNTPs (50 μM), RO-3306 (5 μM) or bortezomib (10 nM). 10 μg/ml resazurin was added for 4 hours and viability was determined (values are normalized to DMSO control), n=2 ± S.E.M.

References

1. Gad H, Koolmeister T, Jemth AS, Eshtad S, Jacques SA, Strom CE, et al. MTH1 inhibition eradicates cancer by preventing sanitation of the dNTP pool. Nature. 2014;508:215-21.

2. Warpman Berglund U, Sanjiv K, Gad H, Kalderen C, Koolmeister T, Pham T, et al. Validation and development of MTH1 inhibitors for treatment of cancer. Ann Oncol. 2016.

3. Kawamura T, Kawatani M, Muroi M, Kondoh Y, Futamura Y, Aono H, et al. Proteomic profiling of small-molecule inhibitors reveals dispensability of MTH1 for cancer cell survival. Sci Rep. 2016;6:26521.

4. Gad H, Mortusewicz O, Rudd SG, Stolz A, Amaral N, Brautigam L, et al. MTH1 promotes mitotic progression to avoid oxidative DNA damage in cancer cells. bioRxiv. 2019:doi.org/10.1101/575290.

5. Rudd SG, Gad H, Sanjiv K, Amaral N, Hagenkort A, Groth P, et al. MTH1 Inhibitor TH588 Disturbs Mitotic Progression and Induces Mitosis-Dependent Accumulation of Genomic 8-oxodG. Cancer Res. 2020;80(17):3530-41.

6. Tsuzuki T, Egashira A, Igarashi H, Iwakuma T, Nakatsuru Y, Tominaga Y, et al. Spontaneous tumorigenesis in mice defective in the MTH1 gene encoding 8-oxo-dGTPase. Proc Natl Acad Sci U S A. 2001;98(20):11456-61.

7. Minocherhomji S, Ying S, Bjerregaard VA, Bursomanno S, Aleliunaite A, Wu W, et al. Replication stress activates DNA repair synthesis in mitosis. Nature. 2015;528(7581):286-90.

8. Beucher A, Birraux J, Tchouandong L, Barton O, Shibata A, Conrad S, et al. ATM and Artemis promote homologous recombination of radiation-induced DNA double-strand breaks in G2. EMBO J. 2009;28(21):3413-27.

9. Bartkova J, Rezaei N, Liontos M, Karakaidos P, Kletsas D, Issaeva N, et al. Oncogene-induced senescence is part of the tumorigenesis barrier imposed by DNA damage checkpoints. Nature. 2006;444(7119):633-7.

10. Halazonetis TD, Gorgoulis VG, Bartek J. An oncogene-induced DNA damage model for cancer development. Science. 2008;319(5868):1352-5.

11. Burrell RA, McClelland SE, Endesfelder D, Groth P, Weller MC, Shaikh N, et al. Replication stress links structural and numerical cancer chromosomal instability. Nature. 2013;494(7438):492-6.

12. Bartkova J, Hamerlik P, Stockhausen MT, Ehrmann J, Hlobilkova A, Laursen H, et al. Replication stress and oxidative damage contribute to aberrant constitutive activation of DNA damage signalling in human gliomas. Oncogene. 2010;29(36):5095-102.

13. Dominguez-Sola D, Ying CY, Grandori C, Ruggiero L, Chen B, Li M, et al. Non-transcriptional control of DNA replication by c-Myc. Nature. 2007;448(7152):445-51.

14. Murga M, Campaner S, Lopez-Contreras AJ, Toledo LI, Soria R, Montana MF, et al. Exploiting oncogene-induced replicative stress for the selective killing of Myc-driven tumors. Nat Struct Mol Biol. 2011;18(12):1331-5.

15. Chen H, Liu H, Qing G. Targeting oncogenic Myc as a strategy for cancer treatment. Signal Transduct Target Ther. 2018;3:5.

16. Miller DM, Thomas SD, Islam A, Muench D, Sedoris K. c-Myc and cancer metabolism. Clin Cancer Res. 2012;18(20):5546-53.

17. Maya-Mendoza A, Ostrakova J, Kosar M, Hall A, Duskova P, Mistrik M, et al. Myc and Ras oncogenes engage different energy metabolism programs and evoke distinct patterns of oxidative and DNA replication stress. Mol Oncol. 2015;9(3):601-16.

18. Kalkat M, De Melo J, Hickman KA, Lourenco C, Redel C, Resetca D, et al. MYC Deregulation in Primary Human Cancers. Genes (Basel). 2017;8(6).

19. Sanjiv K, Hagenkort A, Calderon-Montano JM, Koolmeister T, Reaper PM, Mortusewicz O, et al. Cancer-Specific Synthetic Lethality between ATR and CHK1 Kinase Activities. Cell Rep. 2016;14(2):298-309.

20. Petermann E, Helleday T, Caldecott KW. Claspin promotes normal replication fork rates in human cells. Molecular biology of the cell. 2008;19(6):2373-8.

21. Hahn WC, Counter CM, Lundberg AS, Beijersbergen RL, Brooks MW, Weinberg RA. Creation of human tumour cells with defined genetic elements. Nature. 1999;400(6743):464-8.

22. Zimonjic D, Brooks MW, Popescu N, Weinberg RA, Hahn WC. Derivation of human tumor cells in vitro without widespread genomic instability. Cancer Res. 2001;61(24):8838-44.

23. Grignani F, Lombardi L, Inghirami G, Sternas L, Cechova K, Dalla-Favera R. Negative autoregulation of c-myc gene expression is inactivated in transformed cells. EMBO J. 1990;9(12):3913-22.

24. Puccetti MV, Adams CM, Kushinsky S, Eischen CM. Smarcal1 and Zranb3 Protect Replication Forks from Myc-Induced DNA Replication Stress. Cancer Res. 2019;79(7):1612-23.

25. Campaner S, Amati B. Two sides of the Myc-induced DNA damage response: from tumor suppression to tumor maintenance. Cell Div. 2012;7(1):6.

26. Petermann E, Orta ML, Issaeva N, Schultz N, Helleday T. Hydroxyurea-Stalled Replication Forks Become Progressively Inactivated and Require Two Different RAD51-Mediated Pathways for Restart and Repair. Mol Cell. 2010;37(4):492-502.

27. Kettle JG, Alwan H, Bista M, Breed J, Davies NL, Eckersley K, et al. Potent and Selective Inhibitors of MTH1 Probe Its Role in Cancer Cell Survival. J Med Chem. 2016;59(6):2346-61.

28. Frenzel A, Zirath H, Vita M, Albihn A, Henriksson MA. Identification of cytotoxic drugs that selectively target tumor cells with MYC overexpression. PLoS One. 2011;6(11):e27988.

29. Petermann E, Woodcock M, Helleday T. Chk1 promotes replication fork progression by controlling replication initiation. Proc Natl Acad Sci U S A. 2010;107(37):16090-5.

30. Jones RM, Mortusewicz O, Afzal I, Lorvellec M, Garcia P, Helleday T, et al. Increased replication initiation and conflicts with transcription underlie Cyclin E-induced replication stress. Oncogene. 2012.

31. Bester AC, Roniger M, Oren YS, Im MM, Sarni D, Chaoat M, et al. Nucleotide deficiency promotes genomic instability in early stages of cancer development. Cell. 2011;145(3):435-46.

 doi:10.20944/preprints202208.0369.v1

32. Maya-Mendoza A, Moudry P, Merchut-Maya JM, Lee M, Strauss R, Bartek J. High speed of fork progression induces DNA replication stress and genomic instability. Nature. 2018;559:279-84.

33. Dominguez-Sola D, Gautier J. MYC and the control of DNA replication. Cold Spring Harb Perspect Med. 2014;4(6).